SERIES IN OPTICS AND OPTOELECTRONICS

Holography

Principles and Applications

SECOND EDITION

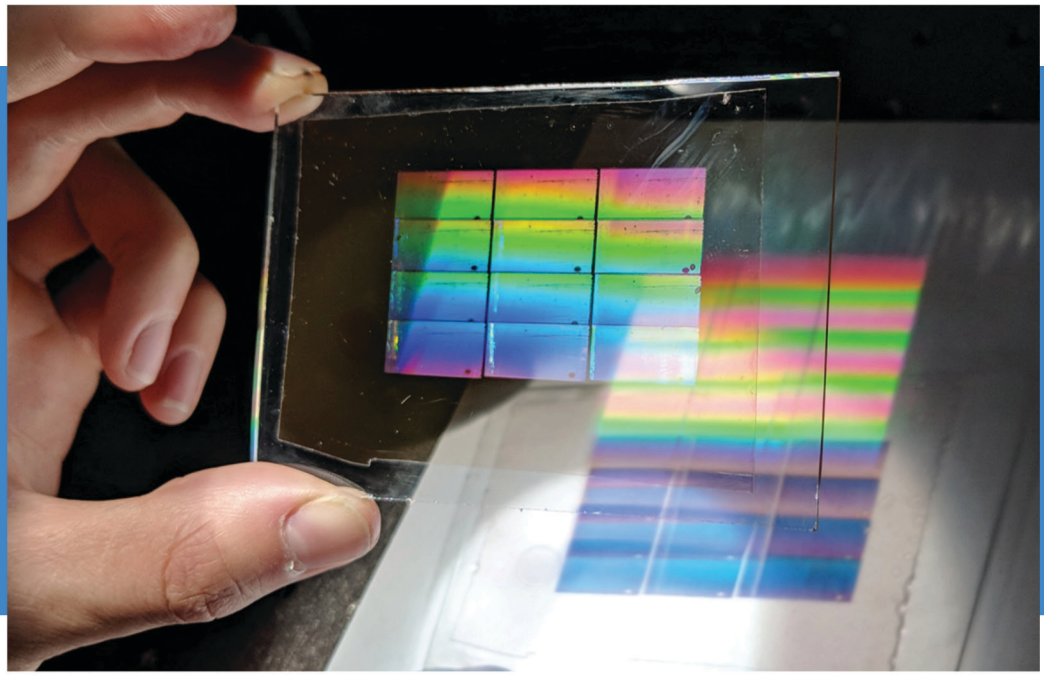

Raymond K. Kostuk

CRC Press
Taylor & Francis Group

Holography

Holography: Principles and Applications provides a comprehensive overview of the theory, practical considerations, and applications of holography. The author has spent his career working on different aspects of this subject and, in this book, conveys the foundation for others to use holography and holographic concepts in a variety of important applications. Special emphasis is placed on the analysis of the imaging and diffraction efficiency properties of holographic optical elements that are finding increasing use in medical imaging, solar conversion systems, and augmented reality eyewear. A comprehensive overview of holographic materials is also given as this area is critical for implementing successful holographic designs. The important areas of digital and computer-generated holography are also presented to give the reader an understanding of these topics. The author has attempted to explain each subject in a manner that he has found effective in teaching holography for over 36 years.

This book is suitable for researchers and as a textbook for graduate students in optics, physics, and engineering. As an aid to instructors and students, the book includes exercise problems and a set of laboratory experiments to enhance understanding. Methods for preparing and handling holographic materials are also provided to help individuals develop experimental capability in holography. In addition, over 470 current and foundational references are provided to help the researcher probe further into this interesting and useful subject.

New Content in the Second Edition:

- Extensive discussion of holographic photopolymers in Chapter 8.
- Extended discussion of holographic optical elements in Chapter 9 with in depth analysis of waveguide coupling HOEs for augmented reality and solar concentrator applications.
- A new Appendix F that covers replication and hologram parameter optimization.
- Revised and extended exercise problems and laboratory experiments with solutions available from the publisher to qualified users.

Raymond K. Kostuk is Professor Emeritus of the Electrical and Computer Engineering Department at the University of Arizona. After completing his military service, he went to Stanford University and earned his Doctorate under the advisement of Professor Joseph W. Goodman working on applying multiplexed holograms to optical interconnect systems. After graduating, he spent a year at the IBM Almaden Research Center where he worked on problems related to optical data storage. He then went to the University of Arizona with a joint faculty appointment in the Electrical and Computer Engineering Department and the College of Optical Sciences. The main focus of his work is on improving holographic recording materials and applying holographic optical elements to various types of optical systems. He has published nearly 100 journal papers, two books, several book chapters, and numerous patents primarily related to different aspects of holography. He is a fellow of the Optical Society of America (now called Optica) and the Society of Photo Instrumentation Engineers (SPIE).

Series in Optics and Optoelectronics

Handbook of Optoelectronics, Second Edition: Concepts, Devices, and Techniques (Volume One)
John P. Dakin, Robert Brown

Handbook of GaN Semiconductor Materials and Devices
Wengang (Wayne) Bi, Haochung (Henry) Kuo, Peicheng Ku, Bo Shen

Handbook of Optoelectronic Device Modeling and Simulation (Two-Volume Set)
Joachim Piprek

Handbook of Optoelectronics, Second Edition (Three-Volume Set)
John P. Dakin, Robert G. W. Brown

Optical MEMS, Nanophotonics, and Their Applications
Guangya Zhou, Chengkuo Lee

Thin-Film Optical Filters, Fifth Edition
H. Angus Macleod

Laser Spectroscopy and Laser Imaging
An Introduction
Helmut H. Telle, Ángel González Ureña

Fourier Optics in Image Processing
Neil Collings

Holography
Principles and Applications
Raymond K. Kostuk

An Introduction to Quantum Optics, Second Edition: Photon and Biphoton Physics
Yanhua Shih

Polarized Light and the Mueller Matrix Approach, Second Edition
José J. Gil, Razvigor Ossikovski

Introduction to Holography, Second Edition
Vincent Toal

Optical Coherence Tomography in Dentistry
Scientific Developments to Clinical Applications
Anderson S. L. Gomes, Denise M. Zezell, Cláudia C. B. O. Mota, John M. Girkin

Holography: Principles and Applications, Second Edition
Raymond K. Kostuk

For more information about this series, please visit: www.crcpress.com/Series-in-Optics-and-Optoelectronics/book-series/TFOPTICSOPT

Holography

Principles and Applications

Second Edition

Raymond K. Kostuk

CRC Press
Taylor & Francis Group
Boca Raton London New York

CRC Press is an imprint of the
Taylor & Francis Group, an **informa** business

Designed cover image: CRC Press

MATLAB® and Simulink® are trademarks of The MathWorks, Inc. and are used with permission. The MathWorks does not warrant the accuracy of the text or exercises in this book. This book's use or discussion of MATLAB® or Simulink® software or related products does not constitute endorsement or sponsorship by The MathWorks of a particular pedagogical approach or particular use of the MATLAB® and Simulink® software.

Second edition published 2025
by CRC Press
2385 NW Executive Center Drive, Suite 320, Boca Raton FL 33431

and by CRC Press
4 Park Square, Milton Park, Abingdon, Oxon, OX14 4RN

CRC Press is an imprint of Taylor & Francis Group, LLC

© 2025 Raymond K. Kostuk

First edition published by CRC Press 2020

Reasonable efforts have been made to publish reliable data and information, but the author and publisher cannot assume responsibility for the validity of all materials or the consequences of their use. The authors and publishers have attempted to trace the copyright holders of all material reproduced in this publication and apologize to copyright holders if permission to publish in this form has not been obtained. If any copyright material has not been acknowledged please write and let us know so we may rectify in any future reprint.

Except as permitted under U.S. Copyright Law, no part of this book may be reprinted, reproduced, transmitted, or utilized in any form by any electronic, mechanical, or other means, now known or hereafter invented, including photocopying, microfilming, and recording, or in any information storage or retrieval system, without written permission from the publishers.

For permission to photocopy or use material electronically from this work, access www.copyright.com or contact the Copyright Clearance Center, Inc. (CCC), 222 Rosewood Drive, Danvers, MA 01923, 978-750-8400. For works that are not available on CCC please contact mpkbookspermissions@tandf.co.uk

Trademark notice: Product or corporate names may be trademarks or registered trademarks and are used only for identification and explanation without intent to infringe.

ISBN: 9781032606187 (hbk)
ISBN: 9781032625409 (pbk)
ISBN: 9781032625423 (ebk)

DOI: 10.1201/9781032625423

Typeset in Minion
by Newgen Publishing UK

Dedicated to
My Wonderful Wife Diane, Daughters Michelle and Marla, Grandson Oakley
and
In Memory of My Parents Walter and Eleanor

Taylor & Francis
Taylor & Francis Group
http://taylorandfrancis.com

Contents

Preface to the Second Edition, xvii

CHAPTER 1 ▪ Introduction and Brief History of Holography 1

1.1 INTRODUCTION 1
1.2 HISTORICAL BACKGROUND 2
1.3 PHILOSOPHY AND CONTENT OF THE BOOK 6

CHAPTER 2 ▪ Background of Physical and Geometrical Optics for Holography 10

2.1 INTRODUCTION 10
2.2 LIGHT AS AN ELECTROMAGNETIC WAVE 10
2.3 POLARIZATION OF AN OPTICAL FIELD 14
2.3.1 Linear Polarization 14
2.3.2 Circular Polarization 15
2.3.3 Elliptical Polarization 15
2.4 COHERENCE 17
2.4.1 Temporal Coherence 17
2.4.2 Spatial Coherence 21
2.5 GEOMETRICAL OPTICS 24
2.5.1 Ray Propagation 24
2.5.2 Reflection at Dielectric Interfaces 25
2.5.3 Optical Lenses 30
2.5.4 Focusing Mirrors 33
2.5.5 Paraxial Rays and Basic Image Analysis Methods 34
2.6 DIFFRACTION ANALYSIS 37
2.6.1 Huygens–Fresnel Formalism of Diffraction 37
2.6.2 Fresnel or Near Field Diffraction Region 39

2.6.3 Fraunhofer or Far-Field Diffraction Region 40
2.6.4 Fourier Transform Properties of a Lens 41
2.6.5 Diffraction by Apertures 43
Problems 45

CHAPTER 3 ▪ Introduction to the Basic Concepts of Holography 49

3.1 INTRODUCTION 49
3.2 HOLOGRAPHIC RECORDING PROCESS 49
3.3 SCATTERING FROM A PERIODIC ARRAY OF POINTS AND THE GRATING EQUATION 52
3.4 HOLOGRAM TERMINOLOGY 54
3.4.1 Diffraction Efficiency 55
3.4.2 Analog, Computer-Generated, and Digital Hologram Recording 55
3.4.3 Thin and Thick (Volume) Holographic Gratings 56
3.4.4 Transmission and Reflection-Type Holograms 57
3.5 HOLOGRAM GEOMETRIES 57
3.5.1 'In-Line' (Gabor Type) Holograms 57
3.5.2 'Off-Axis' Hologram 59
3.5.3 Fourier Transform Hologram 60
3.5.4 Fraunhofer Hologram 62
3.5.5 Hologram Geometry Diagram 63
3.6 PLANE WAVE ANALYSIS OF HOLOGRAMS 63
3.6.1 Grating Vector 65
3.6.2 K-Vector Closure or Bragg Condition 65
3.6.3 Reflection Hologram Example 66
3.6.4 Bragg Circle Diagram 67
3.7 DISPERSION OF *THIN* GRATINGS 69
3.7.1 Example of a Spectrometer with a Holographic Grating 70
Problems 71

CHAPTER 4 ▪ Holographic Image Formation 75

4.1 INTRODUCTION 75
4.2 EXACT RAY TRACING 76
4.2.1 Exact Ray Tracing Algorithm 76
4.2.2 Primary and Secondary Image Formation 81
4.2.3 Forming a Real Image with a Conjugate Reconstruction Beam 81

4.3 HOLOGRAM PARAXIAL IMAGING RELATIONS 82
4.3.1 Analysis of the Phase Distribution from a Point Source to a Hologram Plane 82
4.3.2 Image Magnification Effects 87
4.3.3 Effect of Spectral Bandwidth on Hologram Image Resolution 89
4.4 ABERRATIONS IN HOLOGRAPHIC IMAGING 91
4.4.1 Spherical Aberration Coefficient: 92
4.4.2 Coma Aberration Coefficient 92
4.4.3 Astigmatism and Field Curvature Aberration Coefficients 93
4.4.4 Distortion Aberration Coefficient 93
4.4.5 Example of a Holographic Lens Formed with Spherical Waves and Methods to Reduce Image Aberration 94
4.5 COMPENSATION OF IMAGE SHIFT DUE TO DISPERSION 95
4.6 ANALYZING HOLOGRAPHIC LENSES WITH OPTICAL DESIGN TOOLS 97
4.7 HOLOGRAM FORMATION WITH ASPHERIC WAVEFRONTS 101
4.8 HOLOGRAPHIC LENSES RECORDED AND RECONSTRUCTED AT DIFFERENT WAVELENGTHS 103
4.9 COMBINING IMAGE ANALYSIS WITH LOCALIZED DIFFRACTION EFFICIENCY 104
Problems 105

CHAPTER 5 ▪ Hologram Diffraction Efficiency 108

5.1 INTRODUCTION 108
5.2 FOURIER ANALYSIS OF THIN ABSORPTION AND SINUSOIDAL PHASE GRATINGS 109
5.2.1 Diffraction by a Thin Sinusoidal Absorption Grating 109
5.2.2 Diffraction by a Thin Sinusoidal Phase Grating 111
5.3 COUPLED WAVE ANALYSIS 114
5.3.1 Approximate Coupled Wave Analysis ('Kogelnik' Model) 116
5.3.2 Criteria for Using 'Thin' and 'Thick' Grating Models 142
5.3.3 Rigorous Coupled Wave Analysis 143
5.3.4 RCWA with Special Grating Types 151
5.3.5 Comparison of RCWA with ACWA 152
Problems 156

CHAPTER 6 ▪ Computer-Generated Holograms 161

6.1 INTRODUCTION 161
6.2 PRELIMINARY CONSIDERATIONS FOR THE CGH PROCESS 161
6.2.1 Basic Concept 161
6.2.2 Sampling Continuous Functions 162
6.2.3 Continuous and Discrete Fourier Transform Operations 163
6.2.4 Sampling Requirements at the Object and Hologram Planes 164
6.3 CGH ENCODING METHODS 166
6.3.1 Binary Detour Phase Encoding 167
6.3.2 Binary Interferogram Computer-Generated Holograms 171
6.3.3 Example of a Binary Fourier Transform Hologram 174
6.4 DAMMANN GRATINGS 176
6.5 DYNAMIC CGHS FORMED WITH A SPATIAL LIGHT MODULATOR 179
6.6 CGH DESIGN ALGORITHM OPTIMIZATION METHODS 181
6.6.1 Example of a Gerchberg–Saxton CGH Profile Optimization 182
Problems 185

CHAPTER 7 ▪ Digital Holography 190

7.1 INTRODUCTION 190
7.2 DIGITAL HOLOGRAM PROCESS 190
7.3 DH RECORDING CONSIDERATIONS 191
7.4 CONSTRUCTION GEOMETRIES 193
7.5 RECONSTRUCTION METHODS 196
7.5.1 Fresnel Approximation Method 196
7.5.2 Convolution Method 199
7.6 DIGITAL HOLOGRAM IMAGING ISSUES AND CORRECTION TECHNIQUES 200
7.6.1 Zero-Order Suppression by Background Subtraction 200
7.6.2 Phase Shifting Recording and Correction 201
7.7 APPLICATIONS OF DIGITAL HOLOGRAPHY 203
7.7.1 DH Microscopy 203
7.7.2 Multiple Wavelength DH Microscopy 205
7.7.3 Short Coherence Length DH Microscopy 207
7.7.4 Digital Holographic Interferometry 209
Problems 210

CHAPTER 8 ▪ Holographic Recording Materials 213

8.1 INTRODUCTION 213
8.2 EMULSION-BASED MATERIALS 215
8.2.1 Silver Halide Emulsions 215
8.2.2 Dichromated Gelatin 222
8.3 PHOTOREFRACTIVE MATERIALS 226
8.4 HOLOGRAPHIC PHOTOPOLYMERS 230
8.4.1 Introduction 230
8.4.2 General Photopolymer Composition 230
8.4.3 Grating Formation in Photopolymers 230
8.4.4 Phenanthrenequinone-Doped Poly(Methyl Methacrylate) 235
8.4.5 Commercially Available Holographic Polymer Recording Characteristics and Physical Format 239
8.5 DYNAMIC HOLOGRAPHIC PHOTOPOLYMERS 240
8.5.1 Photorefractive Holographic Photopolymers 240
8.5.2 Holographic Polymer-Dispersed Liquid Crystals 241
8.6 PHOTORESIST MATERIALS 243
8.7 PHOTOCONDUCTOR/THERMOPLASTIC MATERIALS 244
8.8 EMBOSSED HOLOGRAMS 246
8.9 PHOTOSENSITIZED GLASS 246
8.9.1 Sensitized Optical Fiber 246
8.9.2 Photo-Thermo-Refractive (PTR) Glass 247
Problems *248*

CHAPTER 9 ▪ Holographic Optical Elements and Instrument Applications 255

9.1 INTRODUCTION 255
9.2 HOLOGRAPHIC LENSES 255
9.3 HOLOGRAPHIC SPECTRAL FILTERS 260
9.4 HOLOGRAPHIC BEAM SPLITTERS AND POLARIZATION ELEMENTS 266
9.5 SUBSTRATE-MODE HOLOGRAPHIC OPTICAL ELEMENTS 270
9.5.1 Multiplexed Substrate-Mode Hologram Couplers 270
9.5.2 Substrate-Mode Coupling Holograms for Augmented Reality (AR) Applications 272
9.6 VOLUME HOLOGRAPHIC IMAGING 275

9.7 HOLOGRAPHIC OPTICAL ELEMENTS IN SOLAR ENERGY CONVERSION SYSTEMS 282
9.7.1 Holographic Concentrators 282
9.7.2 Light Trapping Holographic Optical Elements 283
9.7.3 Holographic Spectrum Splitting Systems 284
9.7.4 PV Module 'Inactive Area' Collection with Chirped Grating Holograms 288
9.7.5 Other Solar Applications of Holographic Optical Elements 293
9.7.6 Holographic Optical Elements for Agrivoltaics 293
9.8 HOLOGRAPHIC OPTICAL ELEMENTS IN OPTICAL INTERCONNECTS AND COMMUNICATIONS SYSTEMS 296
9.8.1 Optical Interconnects 296
9.8.2 Optical Communications 297
9.8.3 Edge-Illuminated (Edge-Lit) Holograms for Fiber Optic Communications Applications 299
Problems 304

CHAPTER 10 ▪ Holographic Interferometry 311

10.1 INTRODUCTION AND BASIC PRINCIPLES 311
10.2 METHODS FOR FORMING HOLOGRAPHIC INTERFERENCE PATTERNS 312
10.2.1 Double-Exposure Holographic Interferometry 312
10.2.2 Real-Time Holographic Interferometry 313
10.3 MEASURING SURFACE DISPLACEMENTS WITH HOLOGRAPHIC INTERFEROMETRY 314
10.4 SURFACE CONTOURING WITH HOLOGRAPHIC INTERFEROMETRY 315
10.4.1 Multiple Wavelength Surface Contouring 315
10.4.2 Contouring with Two-Point Sources 317
10.5 HOLOGRAPHIC INTERFEROMETRY MEASUREMENT OF REFRACTIVE INDEX VARIATIONS 319
10.6 PHASE SHIFTING HOLOGRAPHIC INTERFEROMETRY 320
10.7 ANALYSIS OF HOLOGRAPHIC INTERFERENCE PATTERNS 321
Problems *321*

CHAPTER 11 ▪ Holographic Displays 324

11.1 INTRODUCTION 324
11.2 REFLECTION DISPLAY HOLOGRAMS 324
11.3 TRANSMISSION DISPLAY HOLOGRAMS 326
11.3.1 Image Plane Holograms 326
11.3.2 Rainbow (Benton) Holograms 327
11.4 COMPOSITE HOLOGRAPHIC DISPLAYS 331
11.4.1 Holographic Stereograms 331
11.4.2 Zebra Imaging Holographic Display 333
11.5 UPDATEABLE HOLOGRAPHIC DISPLAYS 334
11.6 HOLOGRAPHIC COMBINER DISPLAYS 335
11.6.1 Head-Up and Helmet-Mounted Displays 336
11.6.2 Near-Eye Augmented Reality Eyewear 337
Problems *341*

CHAPTER 12 ▪ Holographic Data Storage 344

12.1 INTRODUCTION 344
12.2 HOLOGRAPHIC DATA STORAGE SYSTEM (HDSS) CONFIGURATIONS 345
12.3 HOLOGRAM MULTIPLEXING TECHNIQUES 347
12.3.1 Angle Multiplexing 348
12.3.2 Wavelength Multiplexing 349
12.3.3 Shift Multiplexing 349
12.3.4 Peristrophic Multiplexing 350
12.3.5 Polytopic Multiplexing 352
12.4 RECORDING MATERIAL CONSIDERATIONS 353
12.4.1 Holographic Material Dynamic Range for Multiplexing 354
12.4.2 Hologram Exposure Scheduling 355
12.5 OBJECT BEAM CONDITIONING 357
12.6 REPRESENTATIVE HOLOGRAPHIC DATA STORAGE SYSTEMS 360
Problems *361*

APPENDIX A ▪ Mathematical Relations 365

A.1 SPATIAL FOURIER TRANSFORM OPERATIONS 365
A.2 SOME COMMON FOURIER TRANSFORM PAIRS 366

APPENDIX B ▪ Practical Considerations for Hologram Construction 368

B.1 HOLOGRAPHIC MATERIAL CONSIDERATIONS 368
B.1.1 Change in Film Dimensions (Film Shrinkage, Swelling, or Shearing) 368
B.2 EFFECT OF CHANGES IN AVERAGE REFRACTIVE INDEX AND MODULATED REFRACTIVE INDEX 372
B.3 RELATION OF HOLOGRAM EXPOSURE AND VISIBILITY TO DIFFRACTION EFFICIENCY 373
B.4 EFFECTS OF POLARIZATION AND BEAM RATIO ON HOLOGRAM RECORDING 376
B.5 NOISE GRATINGS 377
B.6 MULTIPLEXED HOLOGRAMS RECORDED IN MATERIALS WITH FINITE DYNAMIC RANGE 380

APPENDIX C ▪ Laser Operation and Properties Useful for Holography 385

C.1 OPTICAL LASER SOURCES 385
C.2 CONDITIONS FOR LASING 387
C.3 TEMPORAL COHERENCE OF A MULTI-MODE LASER 388
C.4 SPATIAL MODES AND GAUSSIAN BEAM PROPERTIES 391
C.5 LASERS COMMONLY USED FOR HOLOGRAPHY 392
C.5.1 Gas Discharge Lasers 393
C.5.2 Ionized Gas Lasers 394
C.5.3 Diode Pumped Solid State (DPSS) Lasers 394

APPENDIX D ▪ Holographic Material Processing Techniques 396

D.1 SILVER HALIDE EMULSIONS 396
D.1.1 Silver Halide Hologram Developers 397
D.1.2 Silver Halide Hologram Fixer Solution 399
D.1.3 Silver Halide Hologram Bleaches 399
D.1.4 Silver Halide Sensitized Gelatin (SHSG) Hologram Processing 401
D.2 DICHROMATED GELATIN EMULSION PREPARATION, EXPOSURE, AND PROCESSING 401
D.2.1 DCG Film Preparation and Exposure Guidelines 402
D.2.2 Basic DCG Development Process 403

D.3 PHENANTHRENE QUINONE-DOPED POLY METHYL METHACRYLATE (PQ-MMA) 404

APPENDIX E ▪ Holography Lab Experiments 406

E.1 LAB 1: TRANSMISSION HOLOGRAMS 406
E.1.1 Handling and Processing Holographic Materials 406
E.1.2 Transmission-Type Holograms 407
E.1.3 Experimental Procedures 407
Questions 408
E.2 LAB 2: TRANSMISSION-TYPE HOLOGRAPHIC LENSES 408
E.2.1 Experimental Procedures 408
Questions 409
E.3 LAB 3: REFLECTION-TYPE DISPLAY HOLOGRAMS 410
E.3.1 Experimental Procedures 410
Questions 411
E.4 LAB 4: HOLOGRAM MULTIPLEXING 411
E.4.1 Experimental Procedures 412
Questions 413
E.5 LAB 5: DIGITAL HOLOGRAPHY 413
E.5.1 Experimental Procedures 413
Questions 415
E.5.2 DH Algorithm 415

APPENDIX F ▪ Techniques for Accurate Fabrication of Volume Holographic Optical Elements 418

F.1 HOLOGRAM REPLICATION METHOD USING MASTER OBJECT AND REFERENCE BEAM HOLOGRAMS AND A PRISM COUPLER 418
F.2 IN-SITU TRANSMISSION HOLOGRAM DIFFRACTION EFFICIENCY MONITORING METHOD 419

INDEX, 427

Taylor & Francis
Taylor & Francis Group
http://taylorandfrancis.com

Preface to the Second Edition

Holography is a very rich field that touches a broad range of disciplines ranging from chemistry to art. The thousands of papers that have been written on this subject since its invention by Dennis Gabor in 1948 underscore this fact. Holography is also part of the public thinking thanks to popularizing the subject through appearance of the Princess Leia hologram in the first *Star Wars* movie, the 'holodeck' in *Star Trek*, and different art exhibits on display around the world. While holographic projections like those that appeared in *Star Wars* and *Star Trek* may not be completely possible, they have stimulated many researchers and engineers toward new types of holographic systems, some of which are discussed in this book.

Technical interest in holography stems from the ability to encode more information about an optical field and optical functionality into a relatively thin recording material. This has led to holographic data storage systems, head-up displays, and point of sale scanners. In the past, one of the difficulties of implementing such applications has been the limitations of recording materials. However, the problem with materials seems to be changing with the advent of new photopolymers that do not require wet processing and do not change their properties during processing. Active recording materials such as photorefractive polymers and polymer-dispersed liquid crystals have also been developed and are finding use in updatable displays and augmented reality eyewear. With the availability of these materials, many new applications of holography are possible.

In addition to research and engineering applications, holography is a great tool for teaching optics because it encompasses a very broad range of optical phenomena. Wave theory, coherence, diffraction, interference, digital and analog optical recording devices and materials, lasers, the list can go on for quite some time. Furthermore, experiments can be performed with inexpensive equipment making lab assignments possible as part of a course. To facilitate this possibility a number of experiments used in my class are included in Appendix E at the end of the book.

Over the years, I have been fortunate enough to work on many projects that apply holographic techniques and designs to different types of optical systems. These included optical interconnects, data storage, imaging, displays, and solar energy conversion. I have also taught a graduate course on holography at the University of Arizona for over

36 years. In writing this book, I have tried to document the concepts found most useful for developing holographic designs and for teaching students. Certainly, most of the ideas were developed by others and hopefully I have given credit to their many contributions. However, in this book I have attempted to explain the different concepts in a manner that has helped students (and me) understand them in a clear and simple manner. In addition, background is provided on many of the projects that our group has researched, especially on holographic optical elements and materials.

Several changes were made to the second edition to improve the organization, depth, and clarity of the first edition. This includes switching Chapters 9 and 11 to introduce holographic optical elements before going into other applications such as displays which now appear in Chapter 11. The discussion of waveguide holographic optical elements is expanded and a more in-depth discussion of their application to augmented reality eyewear and photovoltaic solar energy systems is given. Chapter 8 is expanded to give a more in-depth discussion of photopolymers which has become one of the most important holographic recording materials. Appendix F was added that details a novel hologram replicating method and a technique for making holograms with repeatable diffraction efficiency. Both methods can greatly improve the manufacturability of holographic optical elements, which is important for commercialization. Finally, the problems at the end of each chapter were scrutinized and made clearer, which should be of value to those attempting them. A solutions manual was prepared and is available to instructors and professors.

Preparing a book is a considerable undertaking and requires a great deal of motivation to bring it to completion. For this I would like to thank the help from many of my students at the University of Arizona. Each one has contributed to the knowledge and understanding of different features that are essential to the design and implementation of a successful hologram. A special thanks to my former student Dr. Shanalyn Kemme for her computer-generated hologram example that appears in Chapter 6, and to Dr. Yuechen Wu for his algorithm on digital hologram reconstruction in Appendix E. I have also had the great fortune to be inspired and guided by several of the giants in the field of holography including my graduate research advisor Joseph W. Goodman, Bert Hesselink, Stephen A. Benton, Richard Rallison, Nicholas J. Phillips, Hans I. Bjelkhagen, and Glenn T. Sincerbox, and have tried to include their insight and passion for holography in this manuscript. In addition, I would like to thank many of my colleagues and friends at the University of Arizona including Mark Neifeld, Jennifer Barton, Pierre Blanche, Hyatt Gibbs (deceased), Jack Gaskill (deceased), Nasser Peyghambarian, Masud Mansuripur, Ivan Djordjevic, David Brady, Jerzy Rozenblit, and Bane Vasic. I apologize for any others that I may have omitted. In addition, I would also like to thank Haylie Allan, Caroline Antunes, and Evie Lonsdale at Taylor and Francis for their patients, and a special thanks to Joe Goodman again for inspiration especially throughout my career and during the last year of writing this book.

Finally, a very big thanks to my wonderful wife Diane and my special daughters Michelle and Marla for their unwavering support and encouragement throughout the course of writing this book and in all matters important in life.

CHAPTER 1

Introduction and Brief History of Holography

1.1 INTRODUCTION

The visual effects of holographic images can be quite striking. This results from their three-dimensional nature giving them a lifelike character. Different parts of a scene can appear as the observer changes location similar to what occurs when viewing an object in real life. To illustrate this, consider the images in Figure 1.1 which show two photographs of a hologram taken at two different angles. In the top image, only the woman's left eye can be seen while in the lower image both eyes are visible. The three-dimensional property of a holographic image gives rise to parallax effects and contrasts sharply with images formed by conventional refractive and reflective optical systems.

A refractive or reflective imaging system converts a single object point to a single image point following the conjugate imaging relations as shown in Figure 1.2. In contrast, a hologram can convert a single source point into an entire image.

A hologram is formed in a photosensitive material much like that used for a conventional photograph. However, a photograph only records the intensity of a scene while a hologram records both the intensity and phase of the optical wave coming from an object. Since the photosensitive material used for holography and photography is essentially the same in that it only responds to intensity variations, a method for recording both the intensity and phase of a wave had to be developed. Several important achievements in physics and optics during the 19th and early 20th centuries helped pave the way to achieve amplitude and phase encoding of optical fields and to the demonstration of the first holographic images by Dennis Gabor in 1948 [1].

DOI: 10.1201/9781032625423-1

FIGURE 1.1 The photographs of a hologram taken from two different angles.

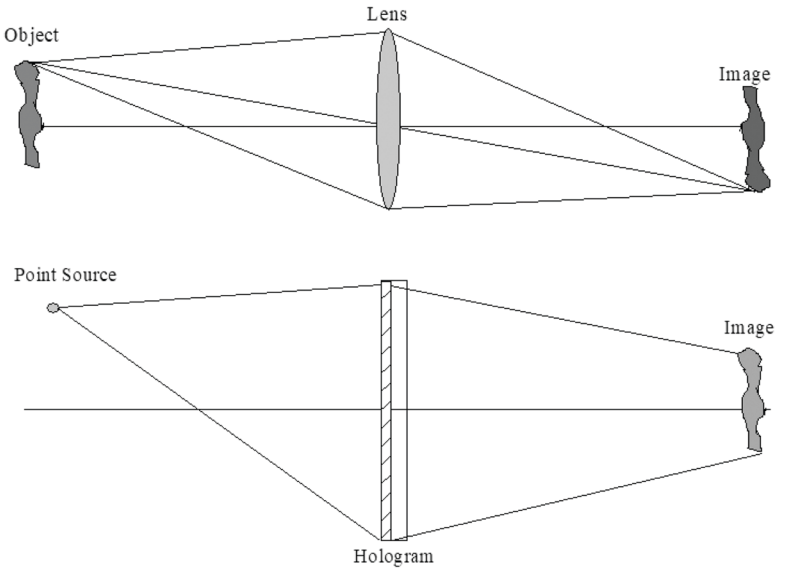

FIGURE 1.2 Contrast between refractive and holographic imaging. The upper figure shows a lens imaging an object and the lower figure shows a hologram transforming light from a point source into an image.

1.2 HISTORICAL BACKGROUND

Dennis Gabor's invention of holography in 1948 [1] was a remarkable achievement (recognized with the Nobel Prize in 1971) that brought together a number of earlier ideas on image formation. The following discussion provides a brief overview of these early efforts. A more comprehensive discussion on the history of holography can be found in reviews by Benton [2], Johnston [3,4], and Richardson and Wiltshire [5]. There is also an enlightening historical perspective in the classic book on holography by Collier, Burkhardt, and Lin [6] and in the book on silver halide materials by Bjelkhagen [7].

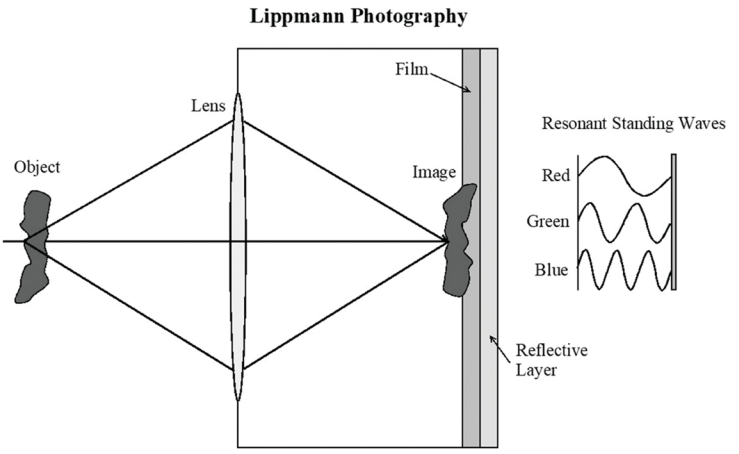

FIGURE 1.3 Lipmann photography setup. An image is formed at the film plane that has a highly reflective backing in close contact. Lipmann originally used a coating of mercury. The reflecting surface sets up standing waves with different wavelengths and results in a color image [7–9].

The following is a synopsis of these more comprehensive histories with some additional anecdotes by the author.

Perhaps the earliest inspiration for holography came from the work by Abbe (1873) who described the formation of an image with a two-step diffraction process [8]. In his analysis, Abbe considers a 'grating like' object illuminated by a plane wave and then imaged by a lens. The lens forms a set of regularly spaced bright spots at the back focal plane of the lens. Each focused spot acts like a point source with spherical waves emanating from secondary sources. The image results from the diffraction pattern formed by the interfering waves from the secondary sources.

During the same time that Abbe was performing his work, other relevant developments in photography were taking place. Most notably was the work of Lippmann who was investigating ways of making color photographs [7,9–11]. He came up with an ingenious method shown in Figure 1.3. Lippmann placed a highly reflective coating on the back surface of an emulsion and then formed a color image on the film with a camera lens. The different color areas set up standing wave patterns in the film. After development the standing wave patterns were converted to localized gratings that filter white light used for viewing and resulted in a color image of the object.

In the early 20th century, Sir Lawrence Bragg pursued the work of Abbe. Bragg was performing research on X-ray diffraction by atomic structures (Figure 1.4) and developed an imaging method by superimposing interference fringes from X-rays scattered by the regularly spaced atoms in crystals on a photographic plate [12]. In some of his methods, accurately placed holes were drilled in a screen at the locations of fringe 'spots' formed by the X-ray interference. If the screen was then illuminated with partially coherent light and imaged through a lens, the optical far-field diffraction pattern on the back focal plane of the lens produced a magnified image of a unit cell of a crystal (Figure 1.5).

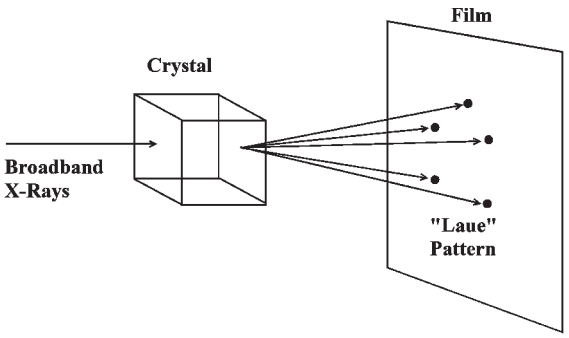

FIGURE 1.4 Bragg diffraction from a crystal forming a 'Laue' pattern on a recording film [12].

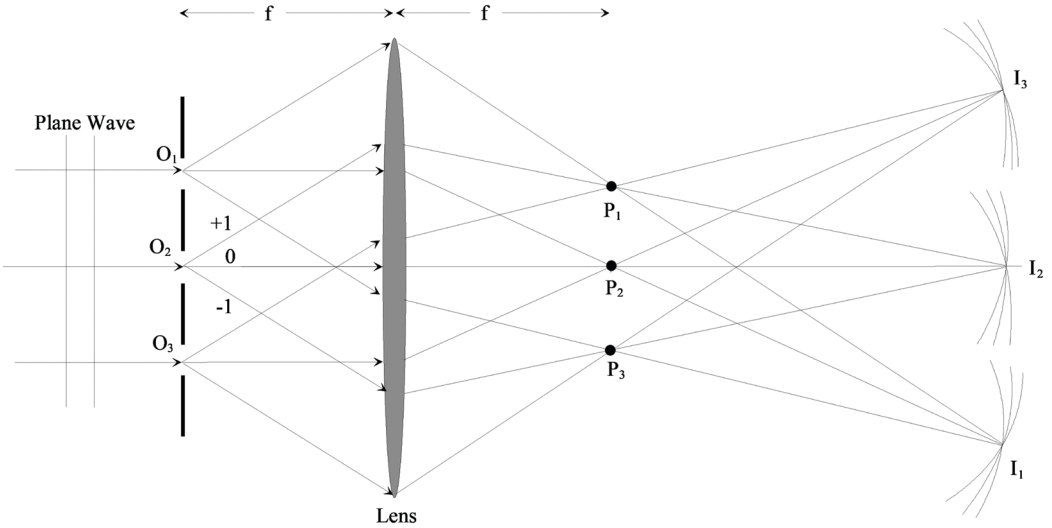

FIGURE 1.5 A depiction of Bragg's method of using Abbe's two-step image formation technique to reconstruct images of crystal lattice structures [6,8].

Gabor recognized Bragg for inspiring his work in his initial paper on holography [13]. At the time of his invention, Gabor was trying to correct aberrations in the lenses used for electron microscopy. He eventually decided to try to use Abbe and Bragg's approach to eliminate the need for the lens altogether. In doing so, he came up with the unique contribution of using coherent light to partially illuminate the object and scatter light. The remaining non-scattered illumination serves as a reference beam that interferes with the object beam, and the interference pattern of the two waves is recorded on a sensitive film. He initially planned to do this recording with the electron beam and then to reconstruct it with an optical beam. However, to demonstrate the method, he performed both the recording and the reconstruction with optical beams and reported this in his seminal paper of 1948 [13]. This was the first demonstration of an optical hologram.

There were however some difficulties with Gabor's initial approach. Since light sources with long coherence length were not readily available, his method was restricted to in-line geometries, which required the object to be highly transparent. Although work continued

on the theory of holography during the 1950s, most notably by H.M.A. El-Sum and A. W. Lohmann [14–16], experimental work did not significantly advance during this time. One important exception was the experiments by G. L. Rogers who also was the first to coin the word 'holography' [17].

A true breakthrough in holography came from Emmett N. Leith and Juris Upatnieks who were working on high-resolution radar imaging at the University of Michigan's Willow Run Lab [18,19] during the early 1960s. Leith had studied Gabor's work and realized the significance of being able to record the phase of an object for imaging applications. He then set out to address the problem of separating the overlapping reconstructed beams that occur with Gabor's in-line hologram geometry. His work resulted in the off-axis hologram geometry that not only eliminated the overlapping reconstruction beams but also allowed holograms to be made of three-dimensional opaque objects. It is interesting to note that holograms made by Leith and Upatnieks were accomplished without the use of a laser. Instead, they used a clever method to extend the coherence length of a mercury discharge lamp with a diffraction grating [6]. Their holograms captured the imagination of both scientists and the public when they displayed a hologram of a three-dimensional object at the Optical Society of America's annual meeting in 1964. Shortly afterward when lasers became readily available, off-axis and true three-dimensional holography was easier to fabricate and generated a great deal of interest and experimentation [20].

Another pioneer of early holography was Yuri Denisyuk from the former Soviet Union. He focused his efforts on the formation of holograms using a reflection geometry [21,22]. Although he was not aware of Gabor's work, he was influenced by the dissertation by El-Sum and Lipmann photography. His efforts resulted in truly exceptional reflection holograms that can be viewed with white light due to the highly selective characteristics of reflection holograms. To achieve high-quality reflection holograms, he helped to develop fine-grain silver halide emulsions capable of resolving up to 10,000 l/mm [23]. For his work on holography, Denisyuk received the Lenin Prize in 1970 which in the former Soviet Union was an award considered comparable to the Noble Prize.

The 1960s also saw a great deal of other work that had a significant impact on the field of holography. In 1963 P. J. van Heerden wrote two papers that outlined the capability of volume holography for holographic data storage (HDS) [24,25] and influenced an entirely new way of thinking of optical storage that continues to this day [26]. In 1965 K. A. Stetson and R. L. Powell demonstrated the technique of interferometric holography for measuring wavelength scale defects and changes in physical surfaces [27,28]. This work has grown into perhaps one of the most widely used applications of holography. (Thomas Kreis has written an excellent text on this subject [29].) In 1967 two important developments in holography occurred. First was the demonstration of digital holography (DH) by Joseph W. Goodman and R. W. Lawrence that optically records an interference pattern with a digital camera [30]. The holographic image is then computationally reconstructed. This has given rise to the advent of digital or electronic holography which has become an area of intense research with the development and availability of high-performance digital cameras. The second contribution in 1967 was the demonstration of computer-generated holograms by A. W. Lohmann and D. P. Paris in which the hologram

is mathematically described and printed in a medium [31]. A holographic image or wavefront is then optically reconstructed. The method allows the recording of objects that are not physically realizable and has been found very useful for testing aspheric optical surfaces [32,33]. In 1969 Steve Benton invented the 'rainbow hologram' which allowed high fidelity viewing of images from transmission holograms with non-laser sources [34]. A key aspect of this design is recognizing that for viewing an object horizontal parallax is more significant than vertical parallax. This allowed him to disperse light from a white light source vertically and view each color band horizontally without degrading image resolution. Finally, one other development during the 1960s was an important paper by Herwig Kogelnik on volume holography [35]. This paper integrated many concepts on diffraction by thick holograms and presented them in a clear and easy-to-understand manner. The concepts in this paper provide a good starting point for analyzing many types of holographic optical elements (HOEs) and Kogelnik's paper is highly cited in subsequent papers on volume holography. Later work on rigorous coupled wave modeling by M. G. Moharam and T. K. Gaylord [36] provided an exact treatment of diffraction by gratings with a variety of physical characteristics. Their work serves as the most general framework for modeling and designing holographic systems and is the basis for many commercial simulation programs. Finally, during the past 10–15 years, the development of new photopolymer recording materials and advances in traditional films such as dichromated gelatin (DCG) has led to a variety of new applications ranging from solar energy collection [37] to augmented reality (AR) displays and eyewear [38,39].

1.3 PHILOSOPHY AND CONTENT OF THE BOOK

The material for this book primarily comes from a graduate course on holography that has been taught for over 30 years at the College of Optical Sciences and the Electrical and Computer Engineering Department at the University of Arizona. Since the main experience of the author has been with volume holography and HOEs, there is a certain bias in the book toward these areas. However, an effort is made to provide an overview of the important areas of holography such as digital and computer-generated holography (CGH) as well as holographic interferometry (HI).

Chapter 2 reviews some of the basic concepts of optics that will be useful in understanding holography. Chapter 3 introduces some of the preliminary ideas of holography and associated terminology used throughout the rest of the book. Explaining the basic ideas at the outset allows more advanced material to be discussed later without the need to step back. The content of Chapter 3 can also be used as a framework for a short course or tutorial on holography.

Chapters 4 and 5 cover respectively two important analytical methods of holography: imaging and diffraction efficiency. The concepts of image formation by holograms are developed from the basic ideas of phase matching through advanced methods of ray tracing, aberration analysis, and optical design. The analysis of hologram diffraction efficiency is considered from several perspectives including the Fourier analysis of thin gratings, approximate coupled wave methods, and rigorous coupled wave analysis. This

provides a suitable framework for analyzing the diffraction efficiency of holograms at several levels.

Chapter 6 describes the basics of CGH. It starts with a review of the sampling criteria necessary for retaining a desired spatial frequency content in the image. This is followed by a discussion of discrete Fourier transform methods that are required for modeling CGH properties. The spatial frequency recording requirements are evaluated for CGHs in both Fresnel and Fourier transform-type geometries. The detour phase hologram encoding method is used as an example to illustrate the process of recording both the phase and amplitude information for CGH. An example of a binary phase interferogram CGH is also provided. This work is followed by a discussion of Dammann gratings and dynamic holograms formed using spatial light modulators.

Chapter 7 covers the subject of DH and builds on the discussion of spatial frequency sampling requirements presented in Chapter 6. Several recording geometries for DH are examined with respect to the required spatial frequency content of the object and digital camera resolution capability. Fresnel and convolution reconstruction methods are discussed as well as techniques to improve imaging quality such as zero-order suppression and phase-shifting recording. The chapter concludes with examples of DH applications including microscopy and interferometry.

Chapter 8 is devoted to holographic materials and is meant to serve as a reference for someone interested either in the study of these materials or with specific holographic application needs. The materials covered include the following: emulsions such as silver halide and DCG; photopolymers for volume hologram recording; photoresists for surface relief type gratings; inorganic and organic photorefractive materials; holographic polymer dispersed liquid crystals; thermoplastics; and sensitized glass fiber and photo-thermo-refractive (PTR) glass.

Chapters 9, 10, 11, and 12 are devoted to holographic applications. Chapter 9 deals with HOEs. This chapter starts with a discussion of holographic lenses and provides a methodology for their design. It then describes the properties of holographic spectral filters, beam splitters, and polarization elements. This is followed by an overview of folded or substrate-mode holographic elements with applications in displays and communication systems. Next, volume holographic imaging (VHI) and its use for subsurface tissue imaging are described as well as its use for the detection of cancer. Following this, the application of HOEs in solar energy conversion is described including holographic solar concentrators, light trapping elements, and spectrum splitting to increase photovoltaic energy conversion efficiency and energy yield. The chapter concludes with an overview of HOE applications in optical interconnects and communications systems such as fiber Bragg gratings and code division multiplexers. Chapter 10 covers the basic concepts of HI including techniques such as double exposure and real-time HI; the measurement of surface displacements, contours, and refractive index variation; phase shifting interferometric methods; and methods for analyzing HI patterns. Chapter 11 deals with holographic displays and includes image plane and reflection holograms, various types of rainbow holograms, multicolor holograms, composite holograms such those developed by Zebra Imaging and stereograms, updateable

holographic displays, heads-up displays, and holograms for AR eyewear. The final main chapter of the book, Chapter 12, deals with HDS. It starts with a description of the basic method of HDS and different recording configurations. This is followed by an overview of the most used multiplexing methods and a discussion of their benefits and limitations. The recording material requirements and the basic metrics for evaluating data storage properties are also given. Techniques for obtaining high-quality HDS including exposure scheduling and object beam conditioning with defocus and phase mask methods are also reviewed. The chapter concludes with a discussion of representative HDS systems.

In addition to the main chapters, six appendices are included to provide some practical background for analyzing, preparing materials, exposing, and processing holograms. These include the following: (A) commonly used Fourier transform algorithms; (B) practical considerations for holographic recording; (C) lasers used for holographic recording; (D) processing and development of commonly used recording materials; (E) a set of holographic experiments suitable for teaching a class on holography or for personal experimentation; and (F) techniques for fabricating HOEs with accurate reconstruction parameters (new for the second edition). Problems and exercises for strengthening concepts and a set of useful references follow each chapter. A solutions manual was also prepared for the problems in the second edition.

REFERENCES

1. D. Gabor, "A new microscope principle," *Nature*, Vol. 161, 777 (1948).
2. S. A. Benton, "Holography reinvented," *SPIE Proc.*, Vol. 4737, 23–26 (2002).
3. S. F. Johnston, "From white elephant to Nobel Prize: Dennis Gabor's wavefront reconstruction," *Hist. Stud. Phys. Biol. Sci. (HSPS)*, Vol. 36, 35–70 (2005); Glasgow ePrints Service, eprints.gla.ac.uk.
4. S. F. Johnston, "Reconstructing the history of holography," *Proc. SPIE*, Vol. 5005, 455–464 (2003).
5. M. J. Richardson and J. D. Wiltshire, *The Hologram: Principles and Techniques*, Ch. 10, Wiley Online Library, Wiley-IEEE Press (2017).
6. R. J. Collier, C. B. Burckhardt, and L. H. Lin, *Optical Holography*, Academic Press, New York (1971).
7. H. I. Bjelkhagen, *Silver-Halide Recording Materials for Holography and Their Processing*, Springer-Verlag, Berlin (1993).
8. E. Abbe, "Beitrage zur Theorie des Mikroskops und der Mikroskopischen wahrnehmung," *Archiv. Mikroskopische Anat.*, Vol. 9, 413–468 (1873).
9. M. G. Lippmann, "La photographie des couleurs," *Comptes Rendus Hebdomadaires des Seances de l'Academie des Sciences*, Vol. 112, 274–275 (1891).
10. M. G. Lippmann, "Photographies colorees du spectre, sur albumin et sur gelatin bichromatees," *Comptes Rendus Hebdomadaires des Seances de l'Academie des Sciences*, Vol. 115, 575 (1892).
11. M. G. Lippmann, "Sur la theorie de la photographie des couleurs simples et composes par la method interferentielle," *J. Physique*, Vol. 3, 97–107 (1894).
12. W. L. Bragg, "The x-ray microscope," *Nature*, Vol. 149, 470 (1942).
13. D. Gabor, "A new microscope principle," *Nature*, Vol. 161, 777 (1948).
14. A. W. Lohmann, "Optical single-sideband transmission applied to the Gabor microscope," *Opt. Acta*, Vol. 3, 97 (1956).
15. H. M. A. El-Sum, *Reconstructed Wavefront Microscopy*, Ph.D. Thesis, Stanford University, Dept. of Physics 1952.
16. H. M. A. El-Sum and P. Kirkpatrick, "Microscopy by reconstructed wavefronts," Phys. Rev., Vol. 85, 763 (1952).

17. G. L. Rogers, "Experiments in Diffraction Microscopy," *Proc. Roy. Soc. (Edinburgh)*, Vol. 63A, 193 (1952).
18. E. Leith and J. Upatnieks, "Reconstructed wavefronts and communication theory," *J. Opt. Soc. Amer.*, Vol. 52, 1123–1130 (1962).
19. E. Leith and J. Upatnieks, "Wavefront Reconstruction with Continuous-Tone Objects," *J. Opt. Soc. Amer.*, Vol. 53, 1377–1381 (1963).
20. R. P. Chambers and J. S. Courtney-Pratt, "Bibliography on Holography," *J. of the SMPTE*, Vol. 75, 373–435 (1966).
21. Y. N. Denisyuk, "Photographic reconstruction of the optical properties of an object in its own scattered radiation field," *Acad. Sci. Rep.*, USSR, Vol. 144, 1275–1278 (1962).
22. Y. N. Denisyuk, "Photographic reconstruction of the optical properties of an object by the wave field of its scattered radiation," *Opt. Spectrosc.*, (USSR), Vol. 14, 279–284 (1963).
23. Y. N. Denisyuk and I. R. Protas, "Improved Lippmann photographic plates for recording stationary light waves," *Opt. Spectrosc.*, (USSR), Vol. 14, 381–383 (1963).
24. P. J. van Heerden, "A new optical method for storing and retrieving information," *Appl. Opt.*, Vol. 2, 387–392 (1963).
25. P. J. van Heerden, "Theory of optical information storage in Solids," *Appl. Opt.*, Vol. 2, 393–400 (1963).
26. K. Curtis, L. Dhar, A. Hill, W. Wilson, and M. Ayres, *Introduction to Holographic Data Recording*, Wiley Online Library, doi: 10.1002/9780470666531, published 30 June 2010.
27. R. L. Powell and K. A. Stetson, "Interferometric vibration analysis by wavefront reconstruction," *J. Opt. Soc. Am.*, Vol. 55, 1593–1598 (1965).
28. K. A. Stetson and R. L. Powell, "Interferometric hologram evaluation of real-time vibration analysis of diffuse objects," *J. Opt. Soc. Am.*, Vol. 55, 1694–1695 (1965).
29. T. Kreis, *Handbook of Holographic Interferometry-Optical and Digital Methods*, Wiley-VCH, Weinheim, 2005.
30. J. W. Goodman and R. W. Lawrence, "Digital image formation from electronically detected holograms," *Appl. Phys. Lett.*, Vol. 11, 77–79 (1967).
31. A. W. Lohmann and D. P. Paris, "Binary Fraunhaufer holograms generated by computer," *Appl. Opt.*, Vol. 6, 1739–1748 (1967).
32. J. C. Wyant and V. P. Bennett, "Using computer generated holograms to test of aspheric wavefronts," *Appl. Opt.*, Vol. 11, 2833–2839 (1972).
33. J. C. Wyant and P. K. O'Neill, "Computer generated hologram: Null lens test of aspheric wavefronts," *Appl. Opt.*, Vol. 13, 2762–2765 (1974).
34. S. A. Benton, "Hologram reconstructions with extended incoherent sources," *J. Opt. Soc. Am.*, Vol. 59, 1545–1546 (1969).
35. H. Kogelnik, "Coupled wave theory for thick hologram gratings," *B. Sys. Tech. J.*, Vol. 48, 2909–2947 (1969).
36. T. K. Gaylord and M. G. Moharam, "Analysis and applications of optical diffraction gratings," *Proc. IEEE*, Vol. 73, 894–937 (1985).
37. R. K. Kostuk, et al., *Holographic Applications in Solar-Energy – Conversion Processes*, SPIE Spotlight, SPIE Press, Bellingham, WA (2016).
38. B. C. Kress and M. Shin, "Diffractive and Holographic Optics as Optical Combiners in Head Mounted Displays," UbiComp'13, 1479–1482, Zurich, Switzerland, Sept. 8–13, 2013.
39. B. C. Kress and T. Starmer, "A review of head-mounted displays (HMD) technologies and applications for consumer electronics," *Proc. SPIE*, Vol. 8720, A–1–A–13 (2013).

CHAPTER 2

Background of Physical and Geometrical Optics for Holography

2.1 INTRODUCTION

This chapter provides a review of the basic principles of physical and geometrical optics that are useful for an understanding of the field of holography. While not completely comprehensive, the material presented here provides the essentials of optics that are needed to understand some of the advanced topics on holography that follow later in the book. For a more comprehensive treatment of the principles of optics, the reader is encouraged to refer to the excellent references at the end of this chapter [1–4].

2.2 LIGHT AS AN ELECTROMAGNETIC WAVE

Light is a part of the electromagnetic spectrum, and the propagation of light can be described by Maxwell's Equations. The general form for these equations is

$$\begin{aligned} \nabla \times \vec{E} &= -\frac{\partial \vec{B}}{\partial t}; \\ \nabla \times \vec{H} &= \frac{\partial \vec{D}}{\partial t} + \vec{J}; \\ \nabla \cdot \vec{D} &= \rho; \\ \nabla \cdot \vec{B} &= 0; \end{aligned} \tag{2.1}$$

where $\vec{E}$ is the electric field vector, $\vec{D}$ is the electric displacement vector, $\vec{B}$ is the magnetic induction vector, $\vec{H}$ is the magnetic field vector, $\vec{J}$ is the electric current density, and ρ is the electric charge density. The symbol $(\times)$ is the vector cross product, $(\cdot)$ is the vector dot product, and $\nabla = \frac{\partial}{\partial x}\hat{x} + \frac{\partial}{\partial y}\hat{y} + \frac{\partial}{\partial z}\hat{z}$ is the vector gradient operator. The fields $\vec{E}, \vec{H}, \vec{B}$, and

DOI: 10.1201/9781032625423-2

$\vec{D}$ are in general functions of both time and space. Several of the field values are related according to

$$\begin{aligned} \vec{D} &= \varepsilon\vec{E} \\ \vec{B} &= \mu\vec{H} \\ \vec{J} &= \sigma\vec{E} \end{aligned} \tag{2.2}$$

where ε is the permittivity, μ is the permeability, and σ is the conductivity (Ohm's law) of the material in which the fields exist with

$$\begin{aligned} \varepsilon &= \varepsilon_r\varepsilon_o \\ \mu &= \mu_r\mu_o \end{aligned} \tag{2.3}$$

ε_r is the relative permittivity and ε_o is the free space or vacuum permittivity. Similarly, μ_r is the relative permeability and μ_o is the free space permeability of the material with

$$\begin{aligned} \varepsilon_o &= 8.854\times10^{-12}\,Farads/m \\ \mu_o &= 4\pi\times10^{-7}\,Henrys/m. \end{aligned}$$

For typical optical materials, $\mu = \mu_o$, $\vec{J}$ and ρ are zero, and Maxwell's equations reduce to

$$\begin{aligned} \nabla\times\vec{E} &= -\mu_0\frac{\partial\vec{H}}{\partial t} \\ \nabla\times\vec{H} &= \varepsilon\frac{\partial\vec{E}}{\partial t} \\ \nabla\cdot\varepsilon\vec{E} &= 0 \\ \nabla\cdot\vec{H} &= 0. \end{aligned} \tag{2.4}$$

For optics, the electric field vector also indicates the polarization direction. To evaluate the basic nature of light propagation, several assumptions must be made and are true for most optical materials. First significant propagation occurs in dielectric materials and many of these materials are *isotropic* meaning that the material has the same properties regardless of the direction of propagation and polarization of the light. (Note that there are birefringent optical materials such as crystals that have different properties but will not be considered at this time.) The material is also considered *homogeneous* in the sense that the dielectric constant does not change as a function of position along the light path. In addition, only light at a single optical frequency or light with a very narrow spectral bandwidth is considered such that the properties of the medium do not appreciably alter the optical frequency. In this sense the material can be assumed to be *non-dispersive*.

With the above assumptions, it is possible to use Maxwell's equations to determine some of the basic propagation characteristics of light. Performing the operation $\nabla\times$ on the first of Equations 2.4 results in

$$\begin{aligned}\nabla\times\left(\nabla\times\vec{E}\right) &= -\mu_o\frac{\partial}{\partial t}\nabla\times\vec{H}\\ &= -\mu_o\varepsilon\frac{\partial^2\vec{E}}{\partial t^2},\end{aligned} \tag{2.5}$$

then applying the vector operator identity

$$\nabla\times\nabla\times\vec{E} = \nabla\nabla\cdot\vec{E} - \nabla^2 E \tag{2.6}$$

and noting that $\nabla\cdot\vec{E} = 0$ for homogeneous materials (i.e. $\nabla\varepsilon = 0$) produces

$$\nabla^2\vec{E} = \mu_o\varepsilon\frac{\partial^2\vec{E}}{\partial t^2} \tag{2.7}$$

which is the wave equation for the electric field. In optics it is more useful to use the refractive index rather than the permittivity, and the two are related through the relation

$$n = \varepsilon_r^{1/2} = \left(\frac{\varepsilon}{\varepsilon_o}\right)^{1/2}. \tag{2.8}$$

Using the refractive index, the wave equation then takes the form

$$\nabla^2\vec{E} = \mu_o\varepsilon_o n^2\frac{\partial^2\vec{E}}{\partial t^2} = \frac{n^2}{c^2}\frac{\partial^2\vec{E}}{\partial t^2} \tag{2.9}$$

where c is the speed of light in vacuum

$$c = \left(\frac{1}{\sqrt{\varepsilon_o\mu_o}}\right). \tag{2.10}$$

A similar result can be derived for the magnetic field vector $\vec{H}$. Equation 2.9 is the wave equation that is commonly used in optics to describe the propagation of the electric field in space and time.

The electromagnetic wave is transverse in the sense that $\vec{E}$ and $\vec{H}$ are perpendicular to each other with

$$\vec{E}\cdot\vec{H} = 0 \tag{2.11}$$

and propagates in a direction given by the Poynting vector where

$$\vec{S} = \vec{E}\times\vec{H}. \tag{2.12}$$

In optics the Poynting vector specifies the direction of the optical ray or the propagation vector $\vec{k}$ with $\vec{k} = k_x \hat{x} + k_y \hat{y} + k_z \hat{z}$, and $\hat{x}, \hat{y}, \hat{z}$ are unit vectors. The components of the propagation vector can also be expressed as

$$k_x = \frac{2\pi n}{\lambda} \cos\alpha,\ k_y = \frac{2\pi n}{\lambda} \cos\beta,\ k_z = \frac{2\pi n}{\lambda} \cos\gamma \tag{2.13}$$

where $\cos\alpha, \cos\beta$, and $\cos\gamma$ are direction cosines that indicate the components of a unit vector in the direction of $\vec{k}$ along the x, y, and z axes respectively as shown in Figure 2.1.

Since the direction cosines are related according to

$$1 = \cos^2\alpha + \cos^2\beta + \cos^2\gamma \tag{2.14}$$

the magnitude of the propagation vector is

$$\left|\vec{k}\right| = \frac{2\pi n}{\lambda} \tag{2.15}$$

One solution to the wave Equation 2.9 is a plane wave. When expressed in Cartesian coordinates a plane wave has the form

$$\vec{E}(x, y, z, t) = E_o \hat{u} \cos\left(\vec{k} \cdot \vec{r} - \omega t + \varphi\right) \tag{2.16}$$

with E_o the amplitude of the field, $\hat{u}$ a unit polarization vector, $\boldsymbol{\omega}$ the radian frequency, $\vec{k}$ the propagation vector, and φ is the optical phase of the field which in general is a function of position. $\vec{r}$ is the distance vector from the origin of the coordinate system to a point on the wavefront (x, y, z). If E_o is a constant, each field component x, y, and z can be represented as a scalar quantity with

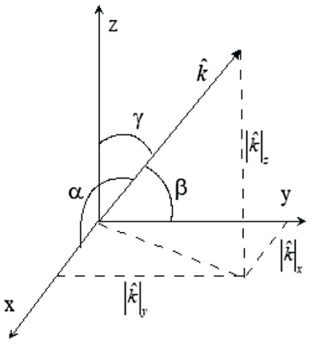

FIGURE 2.1 Propagation vector and components along the x, y, and z directions corresponding to $\cos\alpha, \cos\beta$, and $\cos\gamma$.

. $$E(x,y,z,t) = E_o \cos\left(\vec{k}\cdot\vec{r} - \omega t + \varphi\right) \tag{2.17}$$

For many applications in optics, the scalar field representation is sufficient and provides a simpler solution and greater insight into the problem under investigation than the vector field.

In many cases it is easier to use the complex description of the field to perform different mathematical operations and is given by

$$E(x,y,z,t) = E_o \exp\left[-j\left(\vec{k}\cdot\vec{r} - \omega t + \varphi\right)\right] \tag{2.18}$$

The actual or physical field is the real part of Equation 2.18:

$$E(x,y,z,t) = E_o \exp\left[-j\left(\vec{k}\cdot\vec{r} - \omega t + \varphi\right)\right] \tag{2.19}$$

One advantage of the complex description is that the temporal and spatial factors can be easily separated. If the complex description is substituted into the wave equation (Equation 2.9), the time-dependent component can be dropped to further simplify the expression. In this case, the time independent wave equation is

$$\nabla^2 E + k^2 E = 0, \tag{2.20}$$

which is sometimes referred to as the Helmholtz Equation [5] with

$$E(x,y,z) = E_o \exp\left[-j\left(\vec{k}\cdot\vec{r} + \varphi\right)\right].. \tag{2.21}$$

2.3 POLARIZATION OF AN OPTICAL FIELD

Knowing and controlling the state of polarization of the optical field is important for the formation of holograms. Therefore, a short summary of different polarization states of an optical field is presented in the following sections. A more comprehensive discussion of polarization can be found in references [1] and [6] at the end of this chapter.

As noted in the previous section, the transverse electric field (Equation 2.16) is a time and spatially varying vector and represents the polarization state of the electromagnetic field. The elliptical polarization state is the most general form with linear and circular polarization being important special cases. The description of the polarization state is based on the relative magnitudes of the field components (i.e. E_x and E_y) and the phase difference ($\varphi_{yx} = \varphi_y - \varphi_x$) that exists between them.

2.3.1 Linear Polarization

For linearly polarized light, the tip of the electric field vector moves along a line in a plane transverse to the direction of propagation. If the propagation vector is along the z-axis,

the transverse vectors are in the x and y directions. For this situation, the electric field vector can be expressed as

$$\vec{E}(z,t) = E_{ox}\cos(kz-\omega t)\hat{x} + E_{oy}\cos(kz-\omega t+\varphi_{yx})\hat{y} \tag{2.22}$$

where $E_{ox}\cos(kz-\omega t)$ is the magnitude of the field component in the x-direction and $E_{oy}\cos(kz-\omega t+\varphi_{yx})$ is the field component in the y-direction. $\hat{x}$ *and* $\hat{y}$ are unit vectors in the x- and y-directions, respectively. If the phase $\varphi_{yx} = 2\pi m$ with m = 0, 1, 2 …, then

$$\vec{E}(z,t) = \left[E_{ox}\hat{x} + E_{oy}\hat{y}\right]\cos(kz-\omega t). \tag{2.23}$$

In this case the tip of the polarization vector lies along a line that makes an angle ψ with the y-axis as shown in Figure 2.2 with $\tan\Psi = E_{ox}/E_{oy}$. This situation describes the linear polarization state. If $E_{oy} = 0$, then the field is polarized along the x-axis, and conversely if $E_{ox} = 0$, then the field is polarized along the y-axis.

2.3.2 Circular Polarization

Equation 2.22 can also be used to evaluate other important polarization states. If $E_{ox} = E_{oy}$ and $\varphi_{yx} = (2m-1)\pi/2$ with m = 1, 2, …, then Equation 2.22 can be rewritten as

$$\begin{aligned}\vec{E}_x(z,t) &= E_o\cos(kz-\omega t)\hat{x}\\ \vec{E}_y(z,t) &= E_o\sin(kz-\omega t)\hat{y}\end{aligned} \tag{2.24}$$

The expression can be simplified further by setting $z = 0$. In this case the tip of the electric field vector rotates in a clockwise direction when an observer is at a +z position and is looking back toward the oncoming beam as shown in Figure 2.3.

2.3.3 Elliptical Polarization

If no restrictions are placed on the magnitudes of E_{ox} and E_{oy} or the phase difference $\varphi = \varphi_{yx} = \varphi_y - \varphi_x$, then the x and y field components can be written as

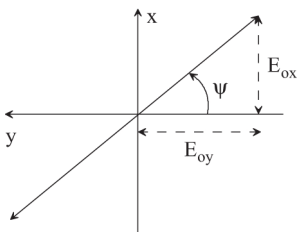

FIGURE 2.2 Diagram showing the path of the tip of the polarization vector for a linear polarized field described by Equation 2.23.

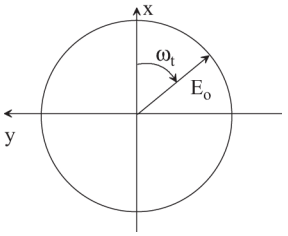

FIGURE 2.3 Rotation of the polarization vector at z = 0 when looking back toward the oncoming beam (i.e. looking in the –z direction from an observation point at z = 0).

$$\begin{aligned} E_x &= E_{ox}\cos(kz-\omega t) \\ E_y &= E_{oy}\cos(kz-\omega t+\varphi). \end{aligned} \tag{2.25}$$

To determine the path traced by the tip of the electric field vector, it will be necessary to eliminate the time and z dependence from Equation 2.25. Rewriting the expression for E_y as

$$\frac{E_y}{E_{oy}} = \cos(kz-\omega t)\cos\varphi - \sin(kz-\omega t)\sin\varphi \tag{2.26}$$

and using $\cos(kz-\omega t) = E_x / E_{ox}$ from Equation 2.25 gives

$$\frac{E_y}{E_{oy}} - \frac{E_x}{E_{ox}}\cos\varphi = -\sin\left(kz-\omega t\right)\sin\varphi. \tag{2.27}$$

Using the identity $\cos^2(\theta)+\sin^2(\theta)=1$ in Equation 2.27 results in

$$\left(\frac{E_x}{E_{ox}}\right)^2 + \left(\frac{E_y}{E_{oy}}\right)^2 - 2\left(\frac{E_x}{E_{ox}}\right)\cdot\left(\frac{E_y}{E_{oy}}\right)\cos\varphi = \sin^2\varphi, \tag{2.28}$$

which is the equation of an ellipse with the primary axis making an angle χ relative to E_x as shown in Figure 2.4 where the tilt angle χ is given by

$$\tan 2\chi = \frac{2E_{ox}E_{oy}\cos\varphi}{E_{ox}^2 - E_{oy}^2}. \tag{2.29}$$

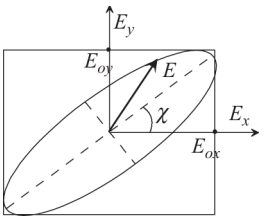

FIGURE 2.4 Diagram showing the path of the tip of the electric field vector $\vec{E}$ for elliptically polarized light.

If $\chi = 0$, then $\varphi = \pm\pi/2$, and Equation 2.29 simplifies to

$$\frac{E_x^2}{E_{ox}^2} + \frac{E_y^2}{E_{0y}^2} = 1 \tag{2.30}$$

Furthermore, if $E_o = E_{ox} = E_{oy}$, then Equation 2.30 describes a circle with E_o equal to the radius.

$$E_o^2 = E_x^2 + E_y^2. \tag{2.31}$$

2.4 COHERENCE

Holography is based on the recording of interference patterns formed by light originating from an optical source. The quality of the interference pattern in turn depends upon the coherence properties of light from the source. Therefore, to optimize the recording of holograms, it is important to understand at least the basic characteristics of coherence.

Two separate forms of coherence can be described: temporal and spatial. Temporal coherence indicates how well the phase difference between two different wavefronts remains at a constant value. In contrast, spatial coherence indicates how constant the phase difference remains across a single wavefront. In this section a review of the basic properties of temporal and spatial coherence is presented. A more complete review of coherence can be found in the text by Goodman on Statistical Optics [7].

2.4.1 Temporal Coherence

Temporal coherence can be expressed as either the length or time that the phase difference between the fields measured at two points along the propagation direction remains essentially constant. The temporal coherence time Δt_c and length Δl_c are simply related by a factor of the speed of light (c)

$$\Delta l_c = c \cdot \Delta t_c. \tag{2.32}$$

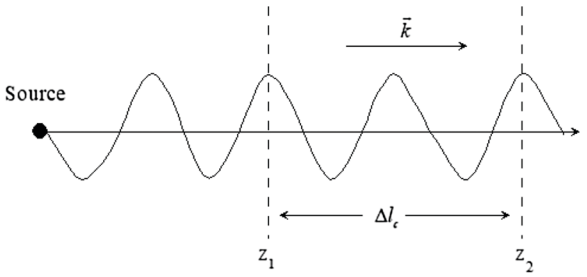

FIGURE 2.5 Diagram of a monochromatic wave with propagation vector $\vec{k}$. The wave is sampled at the points z_1 and z_2 along the direction of propagation.

In addition, for a wave propagating in the z-direction as shown in Figure 2.5,

$$\Delta l_c = z_2 - z_1, \tag{2.33}$$

where z_1 and z_2 are the locations where the phase of the field is sampled.

The correlation between the fields can be quantified by evaluating the interference pattern formed by the fields at the two sampling positions. Assuming that the fields at the sampling locations are given by

$$\tilde{E}_i = E_{o,i} \exp\left[j\varphi_i \right], \quad i = 1,2; \tag{2.34}$$

the power or intensity of the two interfering fields becomes

$$\begin{aligned} I &= \left|\tilde{E}_1 + \tilde{E}_2\right|^2 = \left|\tilde{E}_1\right|^2 + \left|\tilde{E}_2\right|^2 + \left\langle \tilde{E}_1 \tilde{E}_2^* + \tilde{E}_1^* \tilde{E}_2 \right\rangle \\ &= I_1 + I_2 + 2\,\mathrm{Re}\left\langle \tilde{E}_1 \tilde{E}_2^* \right\rangle \\ &= I_1 + I_2 + 2\sqrt{I_1 I_2}\cos(\varphi_1 - \varphi_2), \end{aligned} \tag{2.35}$$

where $\left\langle \tilde{E}_1 \tilde{E}_2^* \right\rangle$ is the time average of the product of the fields. The maximum intensity occurs when $(\varphi_1 - \varphi_2) = 2m\pi$ and a minimum when $(\varphi_1 - \varphi_2) = (2m-1)\pi$, with $m = 0, 1, 2, \ldots$.

Several important situations can now be examined. First if the frequencies of the two fields are different ($\omega_1 \neq \omega_2$), then the time average term in Equation 2.35 becomes

$$\begin{aligned} \mathrm{Re}\left\langle \tilde{E}_1 \tilde{E}_2^* \right\rangle &= \frac{1}{2\Delta t} \int_{-\Delta t}^{\Delta t} \exp\left[-j\left(\omega_1 - \omega_2\right)t \right] dt \\ &= \frac{\sin\left[\left(\omega_1 - \omega_2\right)\Delta t \right]}{\left[\left(\omega_1 - \omega_2\right)\Delta t \right]} \\ &= \frac{\sin\left[2\pi \Delta\nu \Delta t \right]}{\left[2\pi \Delta\nu \Delta t \right]}, \end{aligned} \tag{2.36}$$

where $\Delta\nu = (\omega_2 - \omega_1)/(2\pi)$ is the effective spectral bandwidth of the source. Therefore, a large value for $\mathrm{Re}\left\langle \tilde{E}_1 \tilde{E}_2^* \right\rangle$ will only occur over appreciable time periods when the frequencies are nearly equal. This expression also leads to a useful estimate for coherence given by the product

$$\Delta\nu\Delta t = 1. \tag{2.37}$$

It assumes that the sinc function in Equation 2.36 is a rect function and implies that for sources with large spectral bandwidth, the coherence time will be shorter and conversely.

Quantitative measurements of the temporal coherence length can be made using a Michaelson interferometer as shown in Figure 2.6. In this device an incident beam from the source is collimated and then divided by a beam splitter (BS) sending half the power to two mirrors: M1 and M2. The light is reflected by the mirrors, passes again through the BS, and is combined and displayed on a screen. Initially the mirrors start out at equal distances from the BS ensuring equal optical path lengths (i.e. $z_1 - z_2 = 0$). One of the mirrors is then moved to increase the difference in optical path length between the two beams. If one of the mirrors is tilted, a set of fringes will appear across the screen allowing the maximum and minimum intensity of the interference pattern to be measured. The variation in intensity can be expressed in terms of the visibility defined as

$$V = \frac{I_{\max} - I_{\min}}{I_{\max} + I_{\min}}. \tag{2.38}$$

when V = 1 the source is completely coherent and when V = 0 completely incoherent. Typically, the temporal coherence length is specified at a value less than that corresponding to the distance between the V = 1 and V = 0 visibility locations (i.e. $V = 1/\sqrt{2}$). The distance $\Delta l_c = z_1 - z_2$ where the visibility equals the threshold value is considered the coherence length of the optical source.

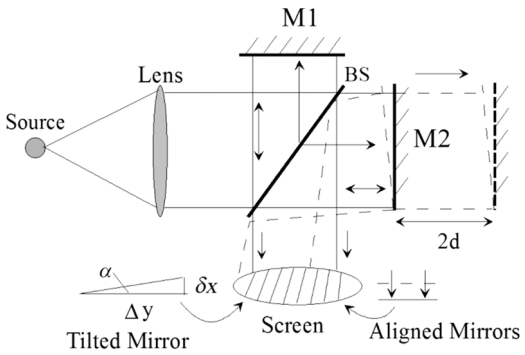

FIGURE 2.6 Diagram of a Michelson interferometer for measuring the visibility of the fringes resulting from sampling the field along the direction of propagation.

Now consider some of the properties of actual optical sources. A purely monochromatic source emits light at a single wavelength or frequency without interruption. This type of source is assumed in describing many optical processes since it makes the analysis simpler. However, no optical source is truly monochromatic as there is always some spectral bandwidth associated with the emission process. The emission of photons from an actual source results from either spontaneous or stimulated processes as shown in Figure 2.7. In both processes an upper energy level is populated with electrons by some means such as optical, electrical, or chemical pumping. Spontaneous emitted photons are randomly released between an upper and lower energy level, while stimulated emitted photons have the same phase and polarization properties as the incident photon. Absorption is a third process related to the photon interaction between two energy bands and is the converse of stimulated emission. This provides a mechanism for populating the upper energy levels (Figure 2.7c).

The upper and lower energy levels consist of a range or band of energy values $\sum_i E_{1,i}$ and $\sum_i E_{2,i}$ that gives rise to many possible energy values for spontaneous emitted photons. Therefore, sources governed by the spontaneous emission process such as light emitting diodes (LEDs) and thermal sources (i.e. incandescent filaments) have a broad spectral bandwidth. In contrast, lasers produce light primarily by stimulated emission and can have a significantly smaller spectral bandwidth. The resulting spectral bandwidth of a laser is also affected by the mechanical stability of the laser cavity that provides optical feedback (see Appendix C).

Two of the most common spectral bandwidth profiles for describing light emission are Gaussian and Lorentzian functions [7]. For modeling purposes, it is also useful to consider a rectangular profile because it illustrates the main relationships source bandwidth and the coherence time and length as given in Equation 2.37. For example, Figure 2.8 shows the power spectrum for a Gaussian and a rectangular distribution. Most of the power is contained within the full width at half maximum (FWHM) bandwidth ($\Delta\nu$) about the center frequency ν_o. Therefore, it is possible to estimate the coherence

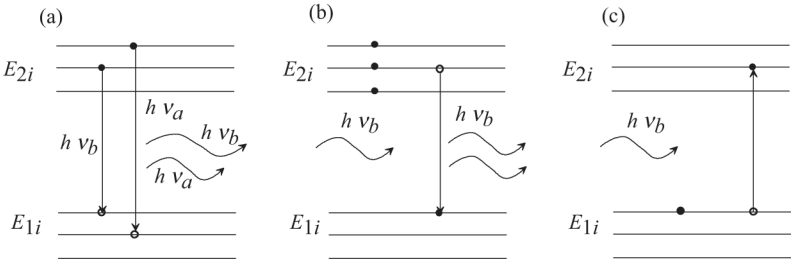

FIGURE 2.7 Diagram of the basic interactions between photons and a material system. (a) Spontaneous emission at multiple wavelengths; (b) Stimulated emission at a wavelength with similar properties as the incident wavelength; and (c) Absorption of an incident photon.

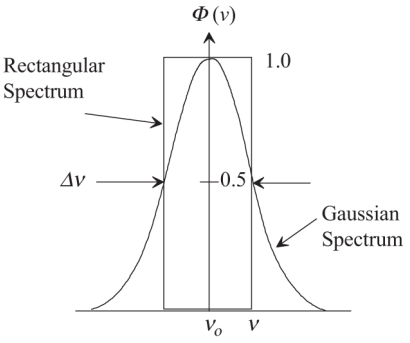

FIGURE 2.8 Power spectrum for a rectangular and Gaussian spectral distribution.

length corresponding to a source with a spectral bandwidth $\Delta\nu$ using the simpler rectangular spectral distribution. The analytical expression for the rectangular power spectrum can be written as

$$\Phi(\nu) = \frac{1}{\Delta\nu} rect\left(\frac{\nu - \nu_o}{\Delta\nu}\right) \tag{2.39}$$

where

$$\begin{aligned} rect(z) &= 1; && |z| < 1/2 \\ &= 1/2; && |z| = 1/2 \\ &= 0; && elsewhere. \end{aligned} \tag{2.40}$$

As shown in Equation 2.34, a source of width $\Delta\nu$ has a coherence time of Δt or a coherence length given by $\Delta l_c = c \cdot \Delta t_c$ (Equation 2.32). This provides a way to make a quick estimate of the coherence length of source simply by knowing the spectral bandwidth which is usually provided by the manufacturer.

2.4.2 Spatial Coherence

As described in the previous section, the temporal coherence of a source is a measure of the correlation of the optical field measured at two points in the direction of propagation. This represents the correlation between different wavefronts of the field propagating from the source. In contrast, the spatial coherence of a source indicates the correlation of the optical field at points across a single wavefront as shown in Figure 2.9. For an extended source (Δx_{src}), rays can reach sampling points P_1 and P_2 by different paths producing a variation in the wavefront. In addition, for a source dominated by spontaneous emission processes, the photons are emitted randomly in time. This causes the phase of the fields reaching the sampling plane to vary. These issues do not exist for a monochromatic point source; however, they must be considered for an extended source such as an LED or the emission region of an arc lamp.

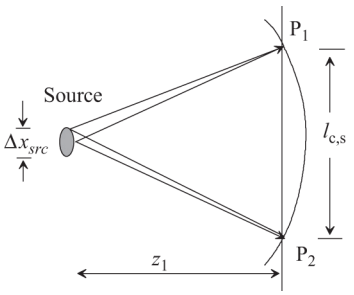

FIGURE 2.9 Diagram showing an extended source and sampling points P_1 and P_2 at a distance z_1 from the source.

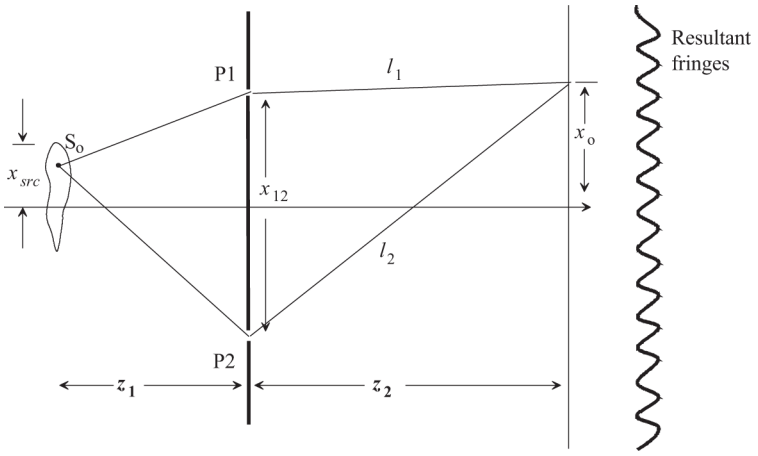

FIGURE 2.10 Diagram of Young's experiment showing sampling the wavefront from an extended source and formation of fringes on an observation plane.

The effects of spatial coherence can be evaluated using the Young's interference experiment as shown in Figure 2.10 [7]. For this experiment it is assumed that the source emits light with a relatively narrow spectral bandwidth at an average wavelength of $\overline{\lambda}$. Light propagates from each point on the extended source (S_o) to an intermediate screen that has two pinholes P_1 and P_2. The pinhole diameters are small in the sense that $\delta_{ph} << z_1\overline{\lambda}/x_{src}$ where δ_{ph} is the diameter of the pinholes and x_{src} is the lateral emission position on the extended source. The length z_1 is the distance between the source and the intermediate screen, and x_{12} is the separation between the two pinholes and determines the locations where the wavefront is sampled. Light that passes through the pinholes propagates to an observation screen located a distance z_2 away and is measured at different positions, x_o, from the optical axis at the observation plane. The sampled light at z_2 results in an interference pattern and can be described by computing the intensity where

$$\begin{aligned} I(x_o) &= \left\langle \left(\tilde{v}_1 + \tilde{v}_2\right)^2 \right\rangle \\ &= \left\langle \tilde{v}_1 \cdot \tilde{v}_1^* \right\rangle + \left\langle \tilde{v}_2 \cdot \tilde{v}_2^* \right\rangle + \left\langle \tilde{v}_1 \cdot \tilde{v}_2^* + \tilde{v}_2 \cdot \tilde{v}_1^* \right\rangle \\ &= I_1 + I_2 + 2\,\mathrm{Re}\left\langle \tilde{v}_1 \cdot \tilde{v}_2^* \right\rangle, \end{aligned} \tag{2.41}$$

where

$$\tilde{v}_1 = \tilde{v}(P_1, t - l_1/c) \text{ and } \tilde{v}_2 = \tilde{v}(P_2, t - l_2/c) \tag{2.42}$$

and represent the fields that propagate through pinholes P_1 and P_2 respectively on the intermediate screen. The time delay for light propagating through the two paths can be combined to form a single parameter

$$\tau = \frac{l_2 - l_1}{c}, \tag{2.43}$$

and used to simplify Equation 2.41 resulting in

$$I\left(x_o, \tau\right) = I_1 + I_2 + 2\,\mathrm{Re}\left\langle \tilde{v}\left(P_1, t + \tau\right)\tilde{v}^*\left(P_2, t\right)\right\rangle \tag{2.44}$$

This result is similar to that found in Equation 2.35 for temporal coherence. In fact, both spatial and temporal coherence properties affect the fringes formed in the Young's experiment. When $\tau = 0$ (i.e. zero path length difference) spatial coherence will dominate fringe visibility. However, when τ becomes large, the fringe visibility decreases due to the reduced degree of temporal coherence.

The combined coherence effects are often expressed using a generalized parameter called the complex degree of coherence [5,7,8] defined as

$$\gamma_{12}\left(\tau\right) \equiv \frac{\Gamma_{12}\left(\tau\right)}{\left[\Gamma_{11}\left(0\right)\Gamma_{22}\left(0\right)\right]^{1/2}}, \tag{2.45}$$

where

$$\begin{aligned} \Gamma_{12}(\tau) &= \left\langle \tilde{v}(P_1, t+\tau)\cdot\tilde{v}^*(P_2, t)\right\rangle, \\ \Gamma_{11}(0) &= \left\langle \tilde{v}(P_1, t)\cdot\tilde{v}^*(P_1, t)\right\rangle, \\ \Gamma_{22}(0) &= \left\langle \tilde{v}(P_2, t)\cdot\tilde{v}^*(P_2, t)\right\rangle. \end{aligned} \tag{2.46}$$

As can be seen the complex degree of coherence is essentially the normalized modulation term in Equation 2.44 (i.e. $2\,\mathrm{Re}\left\langle \tilde{v}(P_1, t+\tau)\tilde{v}^*(P_2, t)\right\rangle$).

However, Equation 2.44 does not fully quantify the constraint that spatial coherence places on the observation region when an extended spatial source is used. This problem was addressed by van Cittert [9] and Zernike [10] using diffraction propagation analysis and other coherence considerations. Their work resulted in a simple relationship [7]

$$A_{coh} = \frac{\left(\bar{\lambda} z\right)^2}{A_{src}} \tag{2.47}$$

where A_{src} is the area of the extended source, $\bar{\lambda}$ is the average emission wavelength, z is the distance between the source and the observer, and A_{coh} is the observation area that has high visibility. The result implies that a smaller extended source area forms a larger region of coherence when observed at a distance *z*. In addition, the further away the observation distance, the larger the coherence region. One example of this is that light from a star has a high degree of spatial coherence.

2.5 GEOMETRICAL OPTICS

The design of holography systems often requires a basic understanding of geometrical optics. Geometrical optics treats the propagation of optical beams as a series of rays that pass through different components such as lenses, mirrors, and BSs. An optical ray indicates the direction of propagation of the optical beam and is the Poynting vector of the optical field described earlier (Equations 2.12–2.13). While a geometrical optics evaluation does not consider physical effects such as diffraction, it provides a great deal of insight into the performance of an optical system. In particular, the pattern of rays on a surface indicates the optical power distribution, and in many cases this information is sufficient for an application. In this section a brief review of several useful principles and relationships of this subject is presented. This discussion provides a basic framework for the design and layout of optical systems that are frequently used for holography. For a more extensive treatment of geometrical optics, the reader is referred to the many texts on this subject some of which are listed in the references [11–13].

2.5.1 Ray Propagation

There are three basic laws of geometrical optics that determine the propagation characteristics of rays through optical materials. These include

1. *Transmission*: The trajectory of a ray remains unchanged in a medium with constant refractive index.
2. *Reflection*: A ray making an angle θ_1 with respect to a surface normal is reflected at an angle θ_2 such that (Figure 2.11a)

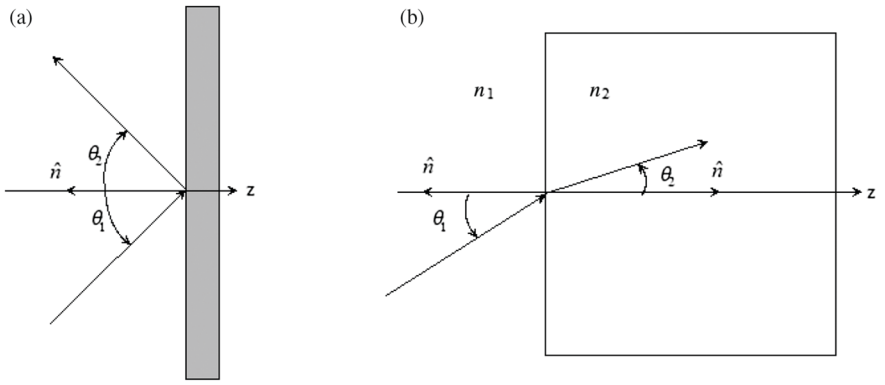

FIGURE 2.11 (a) Reflection of an incident ray at a planar interface. (b) Refraction at an interface with $n_2 > n_1$. z indicates the optical axis for the system.

$$\theta_1 = \theta_2 \tag{2.48}$$

3. *Refraction*: A ray propagating in a medium with refractive index n_1 at an angle θ_1 with respect to a surface normal will be refracted after entering a second material with refractive index n_2 at an angle θ_2 according to Snell's Law such that (Figure 2.11b)

$$\begin{aligned} n_1 \sin\theta_1 &= n_2 \sin\theta_2 \\ \theta_2 &= \sin^{-1}\left[\frac{n_1}{n_2}\sin\theta_1\right]. \end{aligned} \tag{2.49}$$

For both the laws of reflection and refraction, the rays and the surface normal vectors are coplanar. These simple laws are used to describe ray propagation through optical components such as lenses, prisms, BSs, and mirrors. These optical components are made by modifying either the refractive index or reflective properties of surfaces, the surface profile, or the thickness of the component as well as any combination of these parameters.

2.5.2 Reflection at Dielectric Interfaces

2.5.2.1 Fresnel Formulae

As shown in Figure. 2.11b, Snell's Law can be used to determine the direction of a transmitted ray that passes through an interface. However, a more complete description of the interaction of light at an interface is shown in Figure 2.12. The incident power is partially transmitted (T) and partially reflected (R) at the interface with the angle that the transmitted ray makes with the optical axis (z) being described by Snell's Law, and the angle that the reflected component makes with the optical axis described by the Law of Reflection. The field amplitude and power of the reflected and transmitted components can be derived from the boundary matching conditions of the electric and

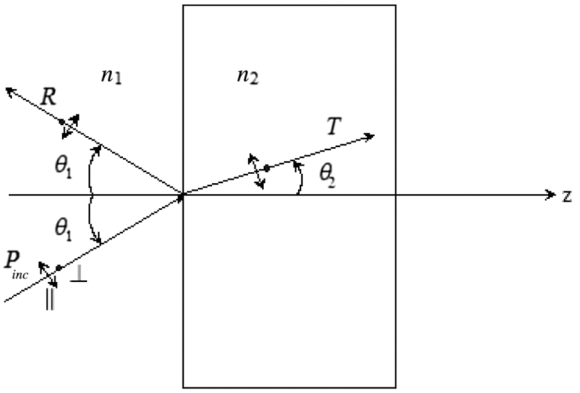

FIGURE 2.12 Diagram showing a ray incident from medium n_1 to n_2 with $n_2 > n_1$. The incident power P_{inc} is partially transmitted and reflected. ⊥ and || indicate the polarization state of the incident beam.

magnetic fields and are called the Fresnel Formulae [1]. Since the field components at the boundary are also a function of the polarization state of the incident beam, there will be a different relation for light polarized in the plane of incidence (p-,||) and perpendicular (s-,⊥) to the plane of incidence.

The resulting Fresnel coefficients for the perpendicularly polarized field component (s-,⊥) are

$$\begin{aligned} r_\perp &= \frac{E_{R\perp}}{E_{inc\perp}} = \frac{n_1\cos\theta_1 - n_2\cos\theta_2}{n_1\cos\theta_1 + n_2\cos\theta_2} \\ t_\perp &= \frac{E_{T\perp}}{E_{inc\perp}} = \frac{2n_1\cos\theta_1}{n_1\cos\theta_1 + n_2\cos\theta_2}, \end{aligned} \tag{2.50}$$

where the angles and refractive index values are shown in Figure 2.12. The corresponding power of the reflected and transmitted components are

$$\begin{aligned} R_\perp &= \frac{P_{R\perp}}{P_{inc\perp}} = \left|r_\perp\right|^2 \\ T_\perp &= \frac{P_{T\perp}}{P_{inc\perp}} = \left(\frac{n_2\cos\theta_2}{n_1\cos\theta_1}\right)\left|t_\perp\right|^2. \end{aligned} \tag{2.51}$$

Note that the transmittance coefficient $T_\perp$ includes an obliquity factor $\left(\frac{n_2\cos\theta_2}{n_1\cos\theta_1}\right)$ and is necessary to ensure power conservation, i.e. $1 = R_\perp + T_\perp$. The Fresnel coefficients for the parallel polarized (p-,||) field components are

$$r_{\|} = \frac{E_{R\|}}{E_{inc\|}} = \frac{n_2 \cos\theta_1 - n_1 \cos\theta_2}{n_1 \cos\theta_2 + n_2 \cos\theta_1}$$
$$t_{\|} = \frac{E_{T\|}}{E_{inc\|}} = \frac{2n_1 \cos\theta_1}{n_1 \cos\theta_2 + n_2 \cos\theta_1}, \tag{2.52}$$

and the corresponding Fresnel coefficients for the optical power are

$$R_{\|} = \frac{P_{R\|}}{P_{inc\|}} = \left|r_{\|}\right|^2$$
$$T_{\|} = \frac{P_{T\|}}{P_{inc\|}} = \left(\frac{n_2 cos\theta_2}{n_1 cos\theta_1}\right)\left|t_{\|}\right|^2 \tag{2.53}$$

These relations show that the amount of light reflected from a dielectric surface can be significant especially if the difference in refractive index between the two materials (n_2–n_1) or the angle of incidence θ_1 are large. If light in air is normally incident on silicon with a refractive index of 3.6, the reflected powers for s- and p-polarized light are both equal to

$$R = \left(\frac{n_2 - n_1}{n_2 + n_1}\right)^2 = 0.32. \tag{2.54}$$

To reduce the large reflection loss, anti-reflection (AR) coatings are often used. In this method layers of dielectric films are deposited on the initial surface to change the phase of the reflected field component. The coatings have a refractive index value (n_c) that are between air with $n_1 = 1.0$ and a substrate with index n_2. Magnesium fluoride (MgF) is often used that has a refractive index of 1.38 and can be deposited by evaporation methods. When the coating layer produces a phase shift of $\lambda_o / 4$ (where λ_o is the free-space wavelength) between the incident and back surface of the film, destructive interference occurs and reduces the reflected intensity. The reflectance from a substrate (n_2) with a single coating layer (n_c) and normal incident light in a medium with index n_1 is [3]

$$R_{AR} = \frac{n_c^2\left(n_1 - n_2\right)^2 \cos^2\left(k_o d'\right) + \left(n_1 n_2 - n_c^2\right)^2 \sin^2\left(k_o d'\right)}{n_c^2\left(n_1 + n_2\right)^2 \cos^2\left(k_o d'\right) + \left(n_1 n_2 + n_c^2\right)^2 \sin^2\left(k_o d'\right)} \tag{2.55}$$

where d' is the optical path length difference between light reflected from the front and back surface of the coating layer and $k_o = 2\pi / \lambda_o$. If the optical path length difference is set to $d' = \lambda_o / 4$, Equation 2.55 reduces to